Deconvolution in Velocity Space

Jon F. Claerbout

ABSTRACT

The deconvolution process is motivated by two phenomena, source signature and near-surface reverberation. Here the process is formulated to include uncertainty in the velocity of near-surface weathered layers. Tests on previously studied data confirm that wave-equation deconvolution removes wide-angle multiples more effectively than does simultaneous pre- and post-NMO deconvolution. No obvious multiple reflections remain. As before, a bubble signature cannot be confirmed as being an essential feature of this data.

Regression coefficients are determined in both offset space and in a velocity space. Regression coefficients determined in the velocity space give better results in offset space than do regressions done entirely in offset space.

INTRODUCTION

An earlier paper, *Simultaneous Pre- and Post-NMO Deconvolution,* in SEP-42 and also submitted to **Geophysics** (alleged to appear in July 1986) asserted that wave theory justifies both pre- and post-NMO deconvolution, but the filters should be estimated *simultaneously,* not *sequentially.* A linearized theory enabled simultaneous estimation of the two filters. Field data test cases showed the expected interaction between NMO and deconvolution. But it was clear that multiple reflection energy remained after the deconvolution. Perhaps that is why the tests were not able to confirm the theoretical concept that simultaneous estimation is superior to sequential estimation. Nor were the tests able to establish any utility of pre-NMO decon when

decon was done after NMO. The difficulties were all ascribed to the inadequacy of NMO as a downward continuation process.

In this paper downward continuation is done with the wave equation instead of NMO. As before, linearized regression still enables handling both designature and dereverberation. Downward continuation is done with a 15° finite-difference program because it offers low noise, dip filtering, and adequate angle bandwidth in near-surface, low-velocity media.

PRE- AND POST-NMO DECON REVIEW

Simultaneous estimation of pre- and post-NMO decon filters (t τ-decon) is embedded in the following model:

$$data \approx \frac{1}{1 - sig} \; \frac{1}{t} \; NMO^{-1} \; \frac{random}{1 - reverb} \tag{1a}$$

First, random white noise is divided by a reverberation filter. (An example of *reverb* expressed in Z-transform notation is $c\ Z^n$ where c is the sea-floor reflection coefficient, and Z^n is the delay operator for vertical travel time). The result is converted into hyperbolas by inverse NMO; a spherical divergence multiplier $1/t$ is applied; and the result is convolved with a source signature wavelet to give the synthetic data. In this model the signature is $signature = 1/(1-sig)$. In this model the same signature wavelet is applied to all offsets, i.e. the source is presumed to be an isotropic radiator.

As an equation for modeling seismograms, (1a) is rather simple. But inversion is more difficult than modeling and (1a) provides a more detailed physical model than underlies conventional deconvolution. My earlier study that used (1a) suggested the most significant factor not incorporated in (1a) is the different moveout velocities of primaries, multiples, and peglegs. The present study generalizes (1a) so that Z is a downward continuation operator. This correctly compensates for the velocity differences.

A MODEL FOR WAVE-EQUATION DECONVOLUTION

A theoretical development has not been prepared. But I imagine it could proceed along the following lines. Modify (1a) to read

$$data \approx \frac{1}{1 - sig} \; \frac{1}{\sqrt{t}} \; \frac{random}{1 - rev \; * \; Diff} \tag{1b}$$

The *NMO* operator has been omitted because the *rev * Diff* operator will now be interpreted as a combination of some regression coefficients and a two-dimensional

diffraction and delay operator. Because the operator is two dimensional, and the real world is three dimensional, there is a remaining $\sqrt{t}$ divergence correction.

Next there should be a linearization step to get a multivariate expression in the unknown regression coefficients of *sig* and *rev*. Then I would make various assertions based on my experience that strict treatment of gain functions is not important. Thus I would conclude that the following regression, which is the one examined by the experimental work in this paper, has a theoretical basis.

$$t^2 \; data(t, x) \quad \approx \quad \sum_i \alpha_i \; Diff(z_i, v_i) \; t^2 \; data(t, x) \tag{2}$$

In this expression, $data(t, x)$ is a field profile, *Diff* is a nonretarded diffraction operator, and α_i is the family of regression coefficients. For each coefficient α_i there is a depth z_i and a velocity v_i. The depth and the velocity will be expressed in a (t, ξ)-plane, where $t = z/v$ is the travel time depth, and $\xi = zv = tv^2$ is the diffraction distance (like the "optical path length"), more generally

$$\xi \;=\; \int v(z) \, dz \tag{3}$$

THE REGRESSORS (figure 1)

Figure 1a shows the marine profile studied. It is profile number 27 from Yilmaz and Cumro [1983] or Yilmaz [in press]. The water bottom depth is about 100ms as is evident by the pegleg interval emphasized by a blank rectangle at 2.5s and 1km offset. The data is displayed (and processed) with a t^2 divergence correction.

Figure 1b shows a typical regressor obtained by delaying the data of figure 1a by the water-bottom vertical two-way time. This panel is used as a regressor onto panel 1a. The coefficient of regression can be placed on a filter at a delay time equal to the travel-time depth. Other panels will also be used in the regression corresponding to other filter lags. Here the filter will be more general, the points being located on a plane, not simply a line (function of lag). The plane is the time-diffraction $(t\ ,\ \xi)$-plane.

Figure 1c shows another regressor. This plane was derived from figure 1a by delay and diffraction to the sea floor. The coefficient for this regressor will be located in the time-diffraction $(t\ ,\ \xi)$-plane at $(t_{bottom}\ ,\ t_{bottom} \times v_{H_2O}^2)$.

The entire time-diffraction plane of regressors was not computed. That would be too many regressors. Remember that each *point* in the time-diffraction plane of regression coefficients corresponds to a plane like figures 1b and 1c. Suppose the water velocity is known but the water depth is not. Then it is sensible to chose regression coefficients as points along a slope of $v_{H_2O}^2$ in the $(t\ ,\ \xi)$-plane. Obviously an ordinary filter is a string of points in the plane along the line of zero diffraction ξ==0. In the present study, delays typically ran from about .75 to about 2.5 times the estimated water depth. This allows for another degree of freedom for a second bounce. Such a model is motivated by knowledge of a more realistic (but much more elaborate) model, namely a surface-consistent model with an independent bounce at the shot and at the hydrophone.

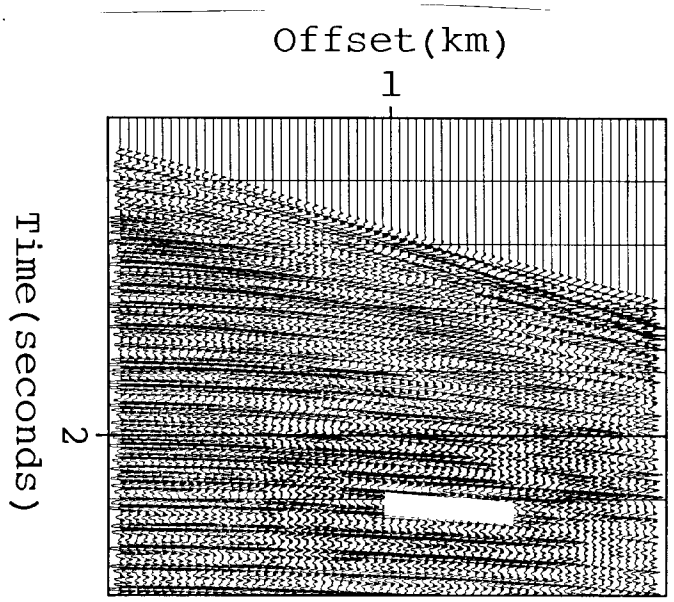

FIG. 1a. Marine profile. The water-bottom depth is measurable by the pegleg interval shown by an overlain white rectangle.

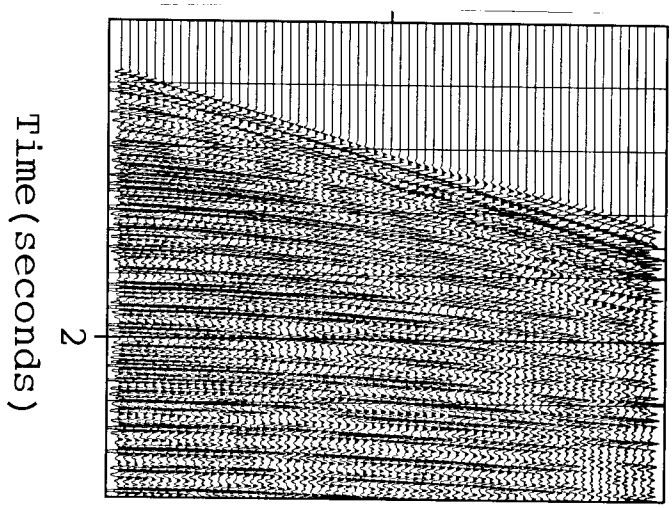

FIG. 1b. The entire profile delayed by the water-bottom vertical two-way time. This panel is used as a regressor on Figure 1a, along with other panels with other delays.

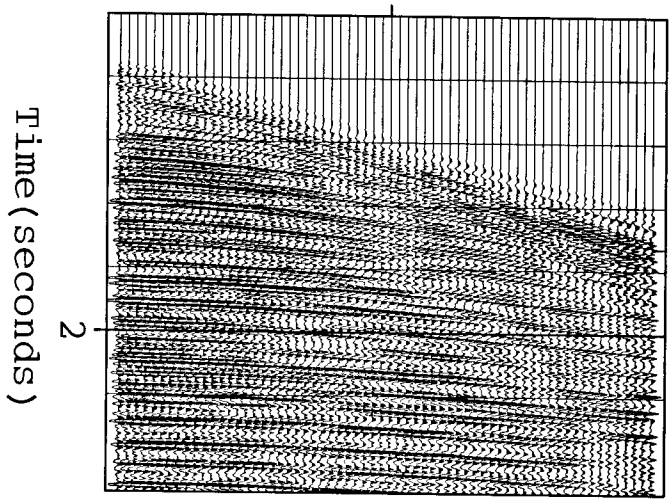

FIG. 1c. Instead of delay like in Figure 1b, this panel was diffracted to the sea floor. An obvious, but irrelevant feature is the absorption of energy around the head wave. The important difference with Figure 1b is the barely perceptible time shift (up) at wide offset. On the far trace it is about a quarter wavelength at latest time and about a half wavelength at 2 sec.

REGRESSION IN VELOCITY SPACE (figure 2)

Ordinarily the regression of the panels of figures 1b and 1c onto 1a is done in the $(t\,,\,x)$ space shown. Ordinarily head waves and direct waves are muted. The high speed of our new Convex C-1 computer allowed me to test another procedure for finding the regression coefficients. The planes of figure 1 were transformed into velocity space and displayed in figure 2.

The horizontal axis on the panels shown is "sloth" or inverse velocity squared. So water sloth $1/1.5^2{=}.45$ is near the right hand edge. The diagonal streaks at early time near the water velocity are from the head waves and direct waves. Observe in figure 2a how the pegleg sequence moves to slower velocities (greater sloths) at later times. This is because the RMS velocity of peglegs decreases from the velocity of the primary.

In velocity space, a window can be placed around events of interest. This was done. Then the regression coefficients can be computed in the window on the velocity space panels in just the same way that the regression coefficients were previously computed on the $(t\,,\,x)$ panels. The advantage of being in velocity space is that a windowing function can select the signal events. It is well known that the effect of noise in a regressor is to give too small a regression coefficient. Putting a window around the real events in velocity space excludes noise. For this data there is not much noise, but never-the-less better results will be seen to arise with the regression coefficients taken from the velocity space.

Ignoring weight functions, it is possible that a regression in the velocity domain would give the same coefficients as a regression in the offset domain. Theoretically, an identical result in each space would seem to depend on some kind of Parseval theorem for velocity space. No attempt was made to establish any such theorem. The topic is raised to stress that different weighting functions apply to different spaces.

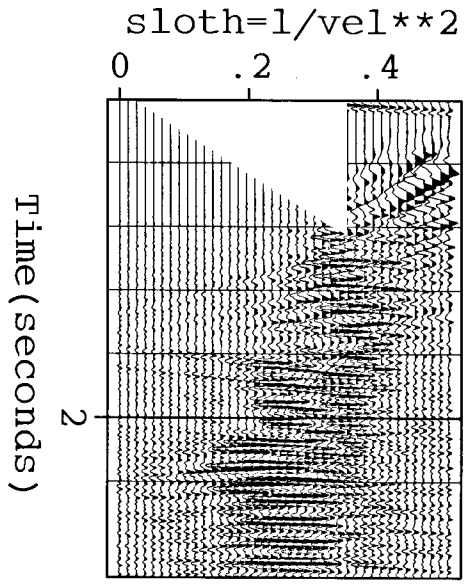

FIG. 2a. Velocity analysis of a field profile. The corner of a triangle marker touches a primary followed by a sequence of peglegs. Two other sequences are also visible. (It is irrelevant that this velocity analysis is "moved out". See *Cable Tangent Stacking,* elsewhere in this report.)

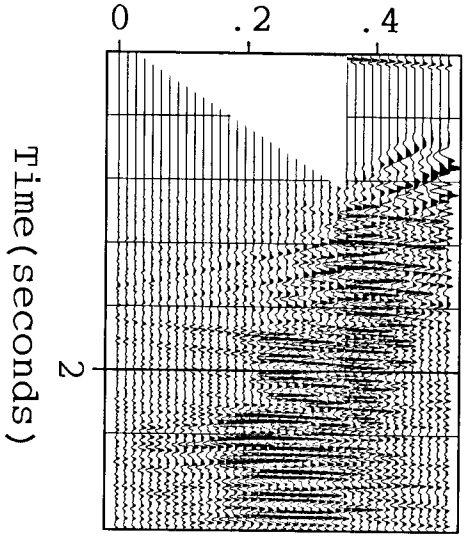

FIG. 2b. The entire profile was delayed by the water-bottom vertical two-way time before velocity analysis. Now the pegleg sequence is delayed as well as shifted from the fixed triangle tip to a lower velocity (higher sloth).

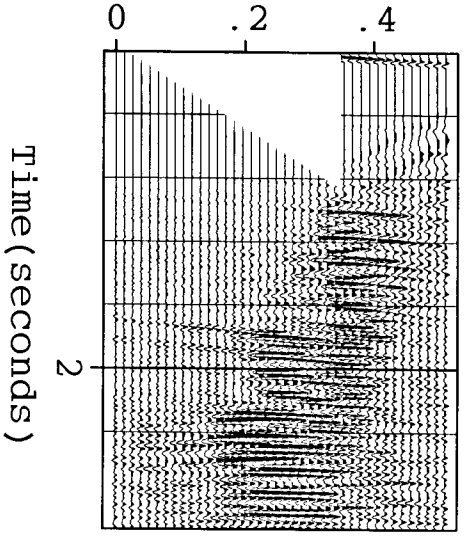

FIG. 2c. Instead of time shifting as in Figure 2b, the profile was diffracted to the sea floor, before the velocity analysis. The pegleg sequences now overlap those of Figure 2a better than do the pegleg sequences of Figure 2b.

FILTERS AS POINTS IN THE $(t\ ,\ \xi)$ PLANE (figure 3)

The "best" $(t\ ,\ x\ )$-space deconvolution is defined to be the plane 1a after planes like 1b and 1c are removed from plane 1a to give minimum power. The "best" $(t\ ,\ \xi)$-space deconvolution is defined likewise with figure 2. As usual I used the Conjugate Gradient Method to do the minimization.

The upper left panel in figure 3 is the original data (after t^2 gain). The best deconvolution is shown in the upper right panel of figure 3. In each of the six panels of figure 3 the $(t\ ,\ \xi)$-planes are plotted directly beneath the $(t\ ,\ x\ )$-planes. At the bottom of the upper right panel you see a $(t\ ,\ \xi)$-plane. Beneath the near trace you see the ordinary designature filter. Along a diagonal line with slope $v_{H_2O}^2$ you see the "wave equation filter," i.e. the regression coefficients, each for a panel such as figure 1c.

The middle two panels in figure 3 are conventional (non wave equation) filter results. You confirm this by inspecting the location of nonzero regression coefficients in the $(t\ ,\ \xi)$-plane. The panel on the left is the result of doing the regression in the $(t\ ,\ x\ )$-domain. On the panel on the right the regression coefficients were determined in the $(t\ ,\ v\ )$-domain of figure 2, and the coefficients were then applied in the $(t\ ,\ x\ )$-domain. Notice that the latter procedure is more effective.

The bottom two panels are a wave equation deconvolution without allowing for a source signature. You confirm this by inspecting the location of nonzero regression coefficients in the $(t\ ,\ \xi)$-plane. The regression coefficients lie along a diagonal line that has the slope of the water velocity squared. On the hard copies it is not evident the velocity space regression coefficients (right side) give a better deconvolution, but the regression coefficients determined in the velocity space seem to be somewhat more clustered about the sea floor and twice the sea floor as predicted by the physical model.

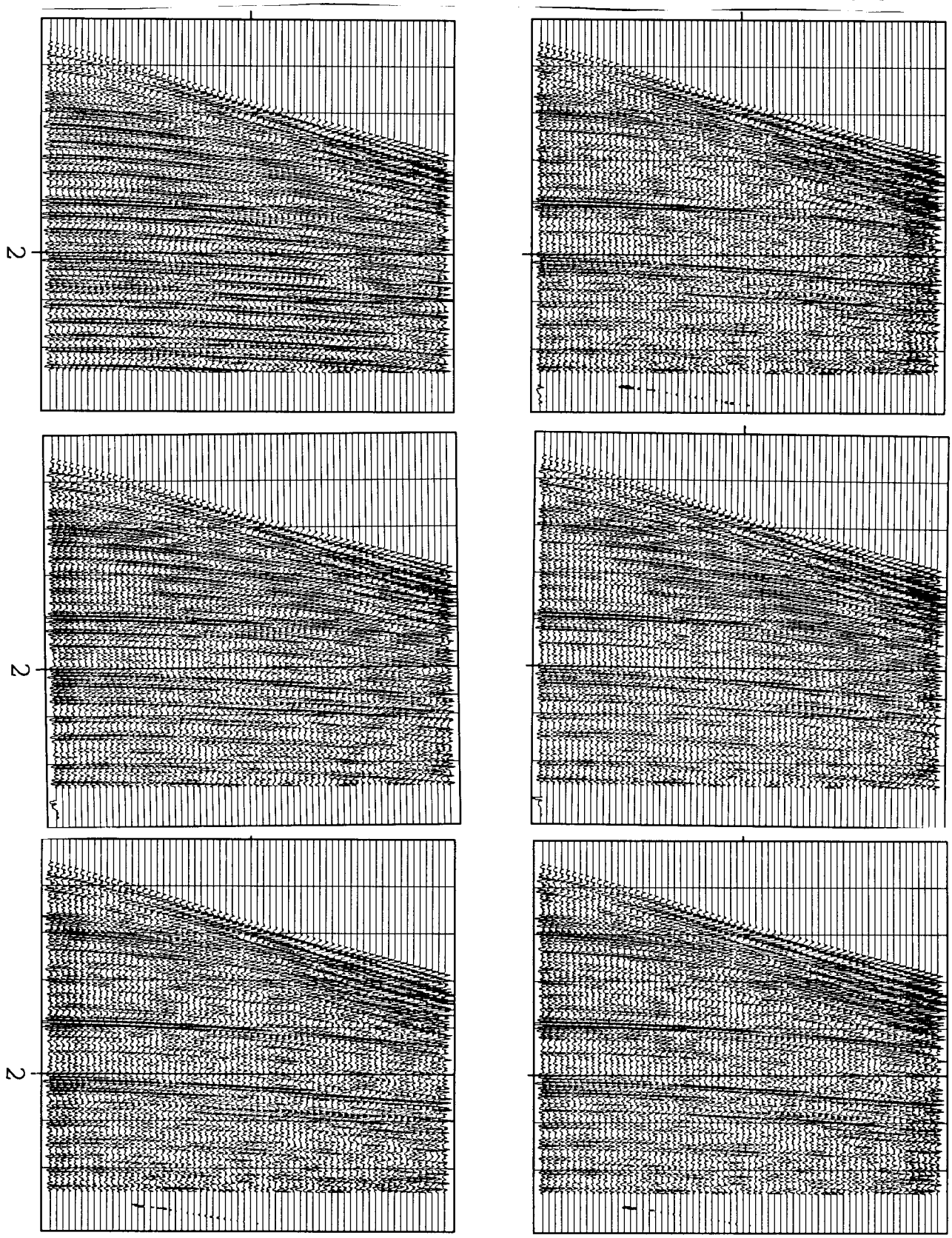

FIG. 3. Profiles each with $(t\ ,\ \xi)$-space filters beneath.

CONVERGENCE SPEED (figure 4)

Viewing on a video display, convergence of the conjugate gradient method seems to take about five iterations. On hard copy as in figure 4, the number five is not so clear. The 6 panels of figure 4 show successively 0,1,2,3,4, and 10 iterations. On these hard copies I see little change in the deconvolved data after the third iteration. However, the filter itself is a little bigger on the tenth than the fourth iteration. This is just more evidence of the superiority of video display.

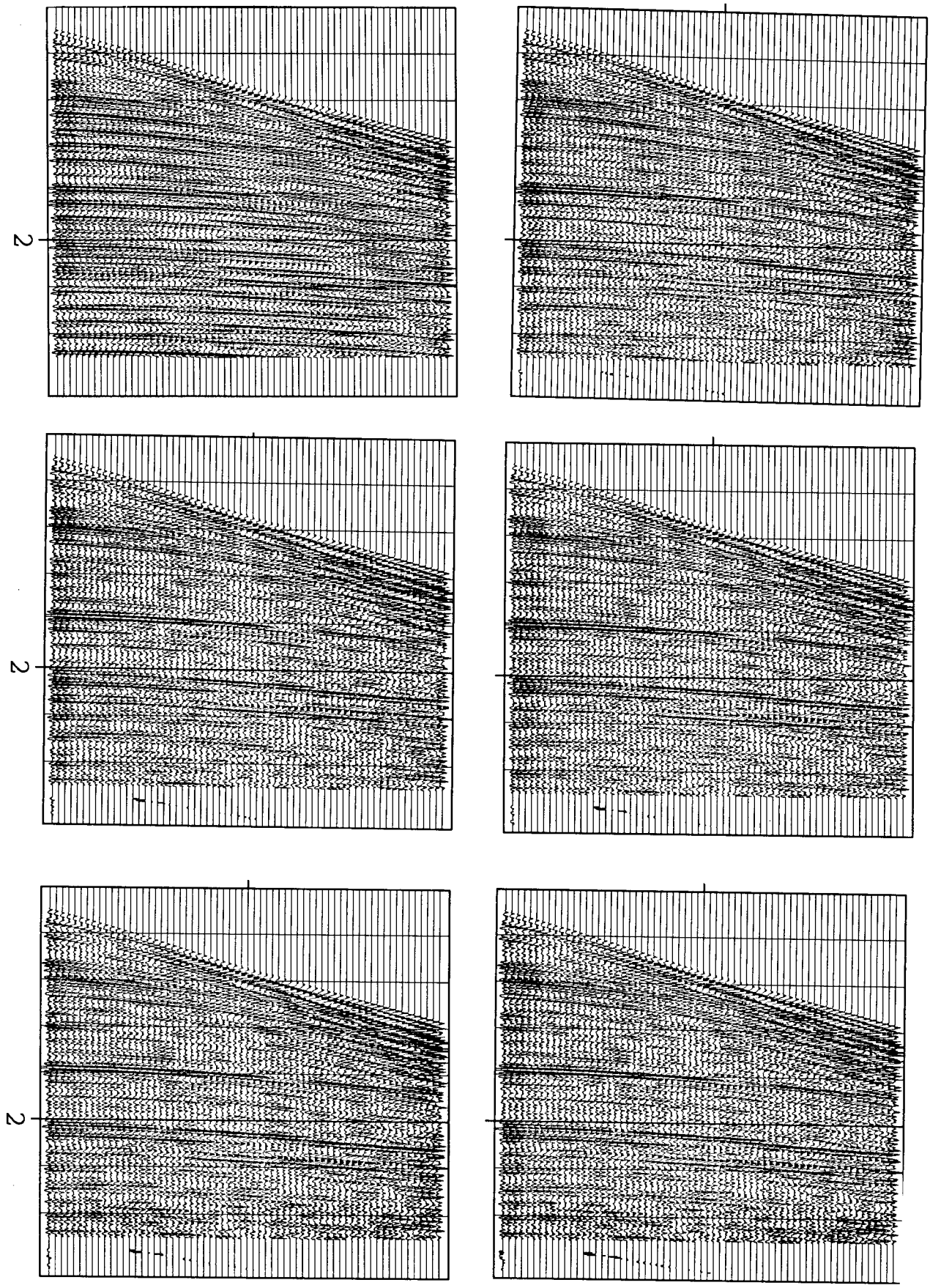

FIG. 4. Iterations 0, 1, 2, 3, 4, and 10.

Figure 5 shows a variety of filter patterns in $(t\ ,\ \xi)$-space. I draw no definite conclusions from the results in figure 5.

CONCLUSIONS SPECIFIC TO THIS DATA SET

1. This wave-equation deconvolution is a textbook case, clearly outperforming decon before and after NMO.
2. From figures 6 and 7, I conclude the model has suppressed all obvious multiple reflections. (Edge diffraction leaves some multiple energy near the near-trace truncation).
3. The raw field profile has extra traces beyond 1.8km that I have not displayed. Their trace spacing happens to be double. The wide spacing causes aliasing for the diffraction program. Such difficulties suggest further theoretical work before more experimental work.
4. Weighting functions in velocity space are worthwhile though it is self evident here only when the operator is crippled by using only convolution (figure 3 middle) and not diffraction (figure 3 bottom).
5. Apparently, the bubble signature is not an essential aspect of the model, i.e. figure 3 upper right is not evidently better than figure 3 lower right.

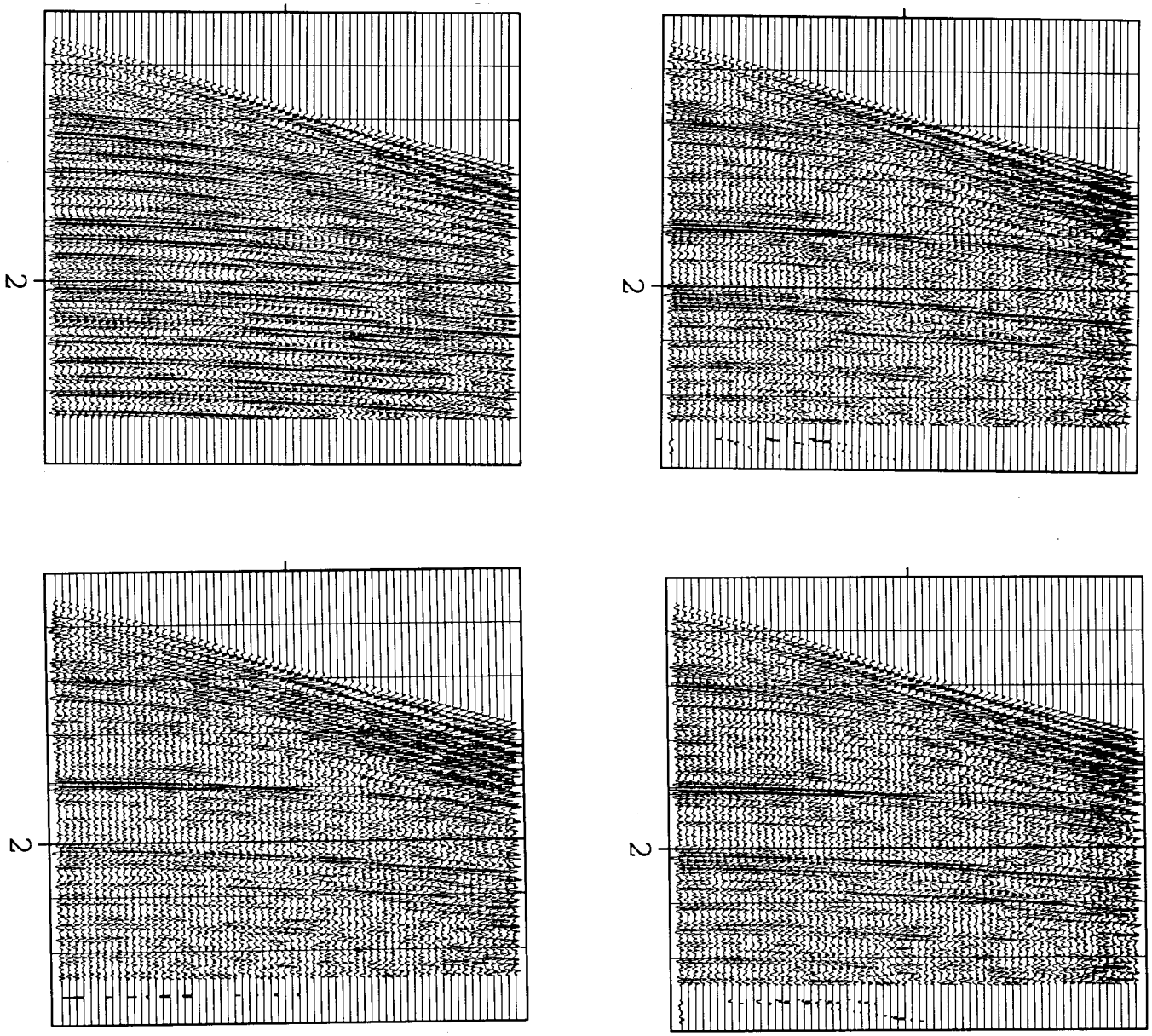

FIG. 5. Some $(t\ ,\ \xi)$-space decons and filters.

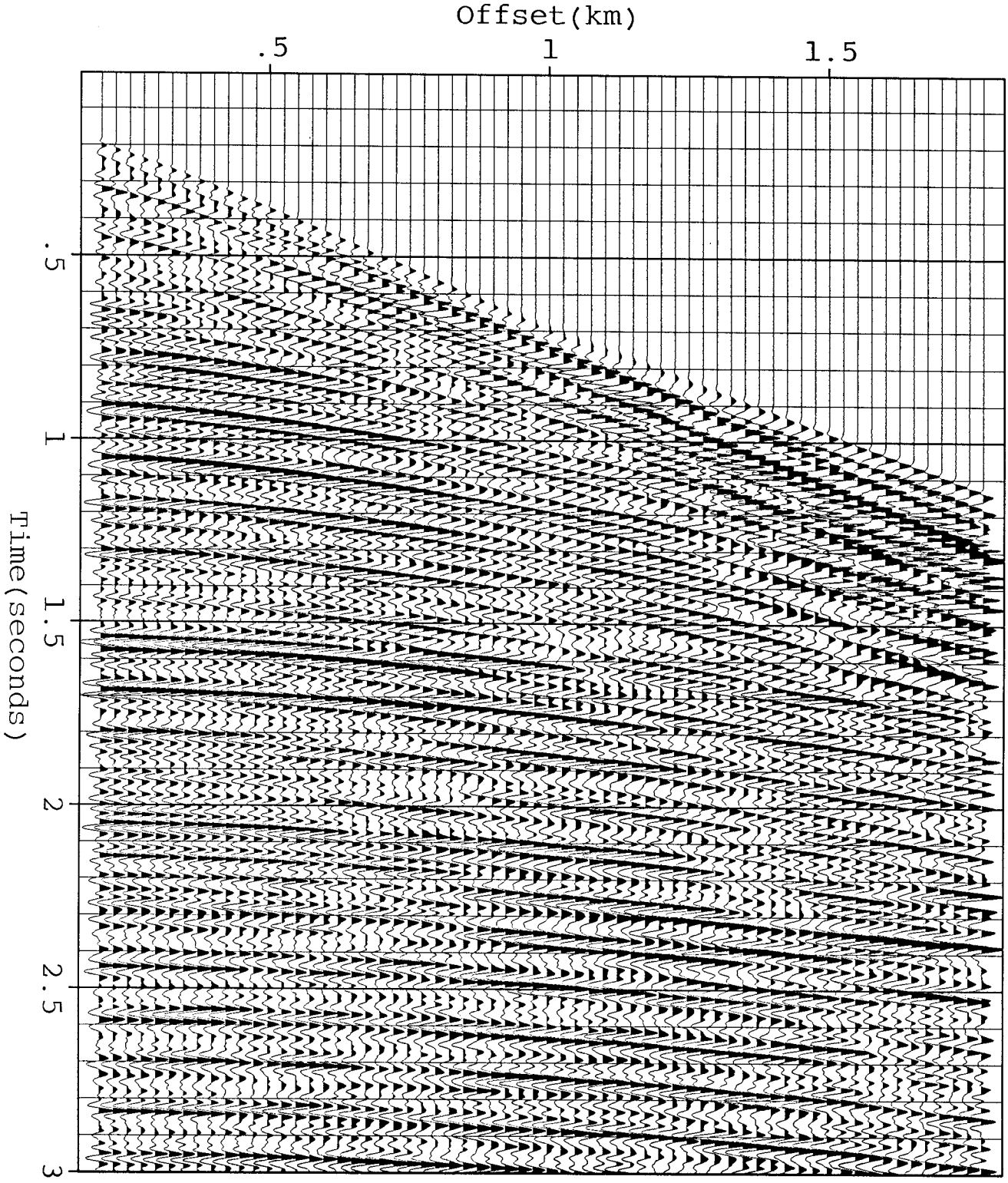

FIG. 6. Expanded plot of test data, i.e. figure 3 upper left.

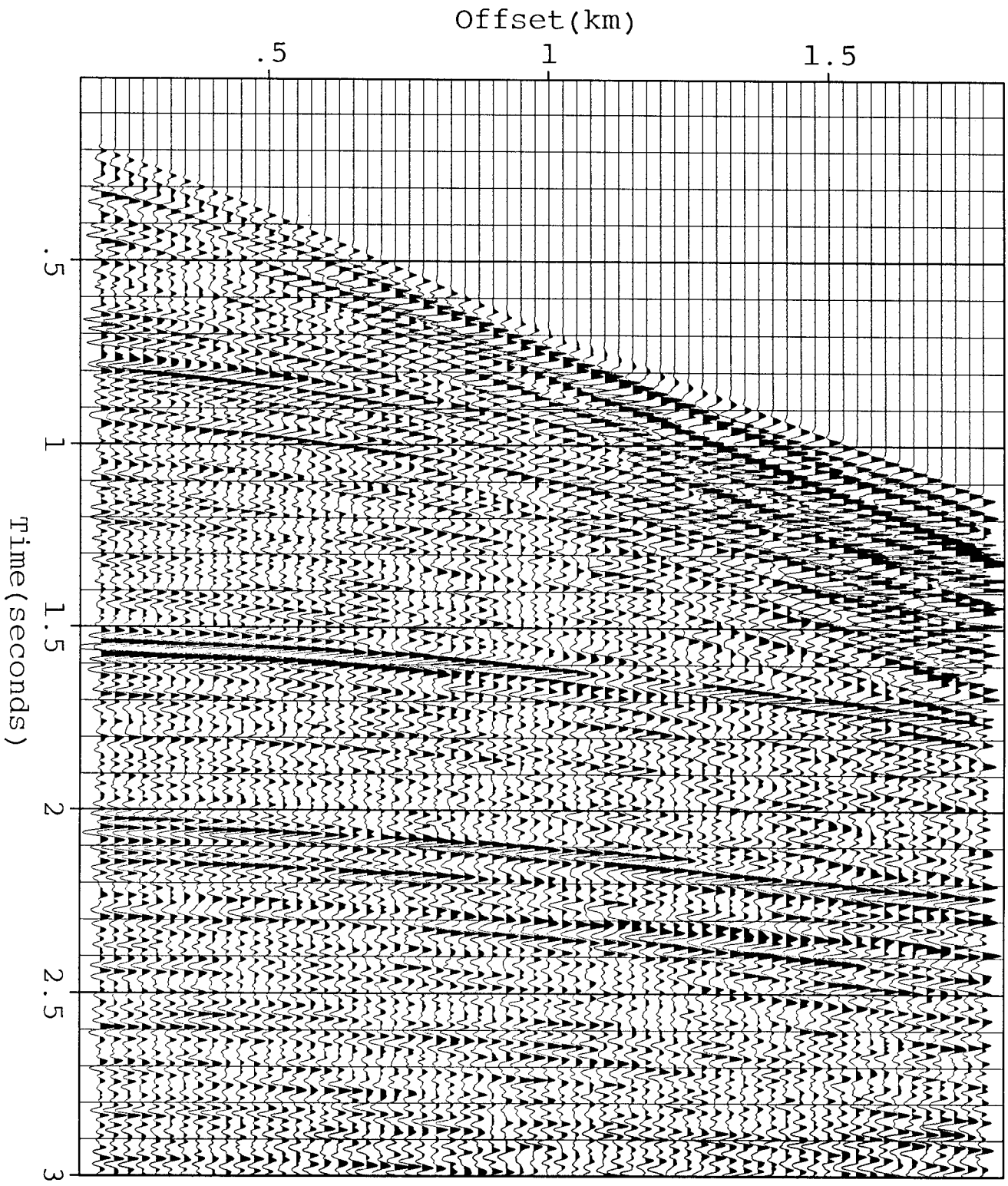

FIG. 7. Expanded best result, i.e. figure 3 upper right. Are there remaining multiples?

POSSIBLE FUTURE DIRECTIONS

1. A more deductive presentation of the regression equations would be appreciated.
2. Theory should encompass weights both in $(t\ ,\ x\ )$-space and in $(t\ ,\ v\ )$-space.
3. The new feature of intelligent handling of weathered layer unknown velocity should be demonstrated in practice, but I am afraid no land data set provides a testbed for deconvolution where the results will be textbook clear. Perhaps with VSP.
4. This program should see more testing than is likely in a university environment.
5. To show the importance of weighting functions in velocity space it should be simply a matter of finding a data set with more noise. The trouble is that few data sets provide textbook quality deconvolutions.

REFERENCES

Claerbout, J., 1985, Simultaneous Pre- and Post-NMO Deconvolution SEP-42, also to appear in Geophysics in July 1986.

Claerbout, J., 1985, Conjugate Gradients for Beginners, SEP-44, p. 161

Yilmaz, O., and Cumro, D., 1983, Worldwide assortment of field seismic records: released by Western Geophysical Company of America.

Yilmaz, O., Seismic Data Processing, in press, Society of Exploration Geophysics, Tulsa